Available online at www.sciencedirect.com
ScienceDirect
Applied Catalysis B: Environmental 80 (2008) 226–236
APPLIED CATALYSIS B: ENVIRONMENTAL
www.elsevier.com/locate/apcatb

The effect of pretreatment on the reactivity of Fe-ZSM-5 catalysts for N_2O decomposition: Dehydroxylation vs. steaming

Pijus K. Roy, Roel Prins, Gerhard D. Pirngruber *

Institute of Chemical and Bioengineering, ETH Zurich, CH-8093 Zurich, Switzerland

Received 4 August 2007; received in revised form 29 September 2007; accepted 4 October 2007
Available online 22 October 2007

Abstract

The N_2O decomposition activity of the Fe-ZSM-5 catalysts, prepared by chemical vapor deposition (CVD) and aqueous ion exchange (IE), was studied after steaming and high temperature treatment at 1218 K (HT) and compared with the activity of the corresponding non-steamed catalysts after pretreatment at 873 K. FTIR spectra showed that dehydroxylation and/or dealumination took place during steaming and high temperature treatment of the catalysts, which leads to the formation of oxygen vacancies (i.e. lattice defect). These lattice defects leads to a change in electronic properties of the iron sites, which are associated with electron withdrawing Al Lewis centers. The iron sites in close proximity of defects are responsible for the initial higher N_2O decomposition (transient activity) of the steamed and HT catalysts. The increase in steady-state activity over steamed and HT catalysts can be mainly attributed to an increase in the number of active sites created by autoreduction of the iron centers during steaming and high temperature treatment. The above-mentioned trends are valid for both CVD and IE samples.
© 2007 Published by Elsevier B.V.

Keywords: Iron zeolite; Isotope labeling; Step response; Dealumination; Defects; Autoreduction

1. Introduction

Fe-ZSM-5 is considered as an interesting catalyst for the decomposition of N_2O, oxidation of benzene to phenol, and selective catalytic reduction of NO_x by ammonia. The activity of the catalyst increases after various treatments of the catalyst at high temperatures. High temperature calcination [1–3] and/or steaming [4–8], and pretreatment in inert gas [9,10], in H_2 [11] or in vacuum [3] are the most common ways to increase the activity of the Fe-ZSM-5 catalysts. The efficiency of different media increases in the sequence air < vacuum ∼ inert gas < H_2 < steam [3]. The question why the pretreatments increase the concentration of active sites and/or the associated reaction pathways [12] remains, as to date, unanswered. The positive effect of steaming and high temperature calcination was first observed for the Fe-ZSM-5 samples prepared by hydrothermal synthesis, which contained Fe in the MFI framework [1,13]. The positive effect of the pretreatment at high temperature was therefore ascribed to the extraction of Fe from an inactive framework position to an active extra-framework position. Later, a positive effect of pretreatments at high temperature was also observed for the samples prepared by ion exchange, which already contained Fe at extra-framework positions [10–15]. The effect of the pretreatments at high temperature is therefore not limited to the extraction of framework Fe. Numerous studies have attempted to explain what happens during the treatment at high temperatures. Kustov et al. provided evidence that the dehydroxylation of Brønsted acid sites at high temperature generates Lewis acid–base pairs, which activate N_2O [2]. According to their work Fe is not involved in the reaction. In view of the overwhelming body of evidence that has meanwhile been collected in support the role of Fe in the activation of N_2O [16,17], this position cannot be upheld any more. If Lewis acidic Al sites are to be involved in the reaction, they must act in combination with Fe. Kauky et al. took up this idea and suggested that an electron-accepting Al Lewis site (created by dehydroxylation at high temperature) in the vicinity of Fe enhances the activity of the latter [18].

For steamed catalysts, slightly different explanations have been forwarded. Hensen et al. suggest that extraframework

* Corresponding author Present address: Institut Français du Pétrole, Department of Catalysis and Separation, F-69390 Vernaison, France.
Tel.: +33 4 7802 2733; fax: +33 4 7802 2066.
E-mail address: pirngruber@chem.ethz.ch (G.D. Pirngruber).

0926-3373/$ – see front matter © 2007 Published by Elsevier B.V.
doi:10.1016/j.apcatb.2007.10.015

Fe–O–Al species are formed by a local amorphisation of the framework [19,20]. The most striking evidence is the observation that the impregnation of a purely siliceous silicalite sample with a mixture of $Fe(NO_3)_3$ and $Al(NO_3)_3$ followed by treatment at high temperatures generates an active catalyst for benzene hydroxylation [21]. The theory of extra-framework Fe–O–Al species is also supported by other groups [22–24]. In contrast, Centi and co-workers claim that hydroxyl nests created by dealumination of the MFI framework play an important role in the reaction [25,26].

Yuranov et al. presented a very interesting comparison of the effect of steaming and dehydroxylation at very high temperatures (1323 K) [27]. They found that behavior of steamed and dehydroxylated samples in N_2O decomposition was qualitatively different and attributed the difference to the formation of mono and bi/oligonuclear iron species by the two methods, respectively. Unfortunately, no spectroscopic characterisation data could be provided to support this argument.

The objective of the present work is to contribute to the ongoing discussion on the effect of high temperature treatment on the catalytic behavior of Fe-ZSM-5. We compare the effect of three different treatments in detail: mild dehydroxylation at 873 K in inert gas, severe dehydroxylation at ~1200 K, and steaming. The study was carried out on catalysts prepared by chemical vapor deposition of $FeCl_3$ (CVD) or by aqueous ion exchange. On these samples the effects of the high temperature treatments are not ''polluted'' by the parallel extraction of framework Fe. For studying the catalytic behavior of the samples in N_2O decomposition, transient response experiments on isotopically labelled catalysts were used. Our results show that the autoreduction of the Fe sites, which increases with increasing pre-treatment temperature [10,28,29], can provide a rather trivial explanation for the positive effect of the high temperature treatment, without the need to invoke structural changes in the catalyst.

2. Experimental

2.1. Preparation of catalysts

The NH_4-ZSM-5 zeolites were obtained from the parent Na-ZSM-5 zeolites (Zeochem, PZ 2-40, Si/Al = 25) by threefold ion exchange with a 1 M NH_4NO_3 solution at room temperature. The NH_4-ZSM-5 was calcined in O_2 (heating rate 1 K/min) at 773 K to convert it into H-ZSM-5.

The iron exchange was carried out by chemical vapor deposition (CVD) of anhydrous $FeCl_3$ on H-ZSM-5 in a flow of N_2 at 593 K, as described elsewhere [10] and calcined in a flow of O_2 at 773 K (1 K/min) for 2 h. This sample is called Fe-ZSM-5 CVD (4.5 wt% Fe). In the second method, the iron exchange was carried out by aqueous ion exchange (IE) of NH_4-ZSM-5 with the iron salt $FeCl_2$*$4H_2O$. About 2 g of NH_4-ZSM-5 was suspended in 40–50 ml of water. To avoid oxidation of Fe^{2+}–Fe^{3+}, the zeolite suspension was degassed with N_2 before adding the iron salt. Then the iron salt was added to the suspension and the solution was refluxed for 5 h at 353 K. After that the solid was filtered, washed with water, dried at 383 K and calcined in air at 773 K for 5 h. This sample is referred as Fe-ZSM-5 IE (0.4 wt% Fe).

Steaming of the calcined sample was performed at a vapor pressure of 30 kPa, a temperature of 873 K (heating rate 10 K/min), for 5 h. The suffix 'st' is used to indicate that the sample was steamed. The high temperature treatment of the Fe-ZSM-5 IE catalyst was carried out at 1218 K (10 K/min) in a flow of He for 2 h. This sample is referred as Fe-ZSM-5 IE-HT.

2.2. Catalyst characterization

Powder X-ray diffraction (XRD) patterns of the parent and iron loaded zeolites after various treatments were recorded from 5 to 50° 2Θ on a STOE DARMSTAD powder diffractometer using Cu Kα radiation and Ge (1 1 1) monochromator at a step size of 0.03°. The powder samples were introduced into a 0.3 mm diameter capillary, which was rotated continuously during the measurement. The diffuse reflectance UV–vis spectra were measured at room temperature on a Cary 400 Scan UV–vis spectrometer (Varian) equipped with a Praying Mantis sample stage from Harrick. $BaSO_4$ was used as a reference. Infrared (FTIR) spectra were recorded in transmission mode at 473 K on a Bio-Rad Excalibur FTS 3000 IR spectrometer equipped with a MCT detector at a resolution of 4 cm^{-1}. Samples were pressed in self-supported pellets of 3–5 mg and degassed at 673 K in He in order to remove adsorbed water. The spectra were then recorded in transmission mode at 473 K; 128 scans were accumulated at a resolution of 4 cm^{-1}. The spectra were normalized using the intensities of the overtone bands of the T–O–T lattice vibrations at 1874 and 1990 cm^{-1}.

2.3. Steady-state N_2O decomposition

The steady-state N_2O decomposition activity was measured after pretreatment of the catalyst at either 773 or 873 K in He for 1 h. An amount of 50 mg palletized catalyst (mesh size 250–300 μm) was first treated in a flow of 10% O_2 in He at 673 K to remove adsorbed impurities and subsequently heated to 773 or 873 K in He. Finally, the catalyst was cooled to 573 K in He and 2500 ppm N_2O in He was fed to the catalyst. The flow over the reactor was kept at 50 ml_{NTP}/min, corresponding to a gas hour space velocity (GHSV) of 40,000 h^{-1}. The decomposition of N_2O was followed for 30 min at each temperature before increasing the temperature by 25–50 K, up to a maximum temperature of 823 K. Gas chromatography was used to detect N_2, N_2O, and O_2. The product gases were analyzed three times at one temperature and an average value was taken for the evaluation of the activity data. The first order rate constant (k) and the activation energy (E_a) were calculated from the following equations:

$$k = \frac{-\ln(1-x)F}{m_{cat}\,p} \quad (1)$$

$$E_a = \frac{\partial(\ln k)}{\partial(1/T)} \quad (2)$$

where x is the conversion, F is the total flow through the reactor, p is the total pressure, m_{cat} is the amount of the catalyst and T is the temperature. The activation energy was determined from an Arrhenius plot (Eq. (2)). Depending on the temperature range chosen for its determination, E_a may vary by ±10 kJ/mol. This value may be considered as the error margin of E_a.

2.4. Step response experiments on isotopically labeled catalysts

Step response experiments were carried out on isotopically labeled catalysts. Fifty milligrams of pelletized catalyst was first treated in a flow to 10% O_2 in He at 673 K in order to remove adsorbed impurities. For the incorporation of ^{18}O into the Fe-ZSM-5 sample, the catalyst was reduced in a mixture of 20% H_2 in He at 673 K for 1 h. This leads to a complete reduction to Fe^{2+} [30]. The step response of the catalyst was carried out after pretreatment at either 673 or 873 K in He. Pretreatment at 673 K was performed as follows: The reduced catalyst was reoxidized at 673 K with 1% $^{18}O_2$ (93% ^{18}O, Eurisotop) in He for 1 h. Then, the catalyst was flushed with He for 10 min at 673 K before step to N_2O. Pretreatment at 873 K was performed as follows: After 30 min at 673 K in a flow of 1% $^{18}O_2$ in He, the catalyst was heated to 873 K (heating rate 6 K/min) in the same flow and kept in $^{18}O_2$ for 5 min and then for another 1 h or 10 min (for Fe-ZSM-5 IE-HT catalyst) in He at 873 K. Finally the catalyst was cooled to 673 K in He. Then, a step to 5000 ppm N_2O in He was performed.

The gas flow rate over the reactor was always kept at 25 ml_{NTP}/min, corresponding to GHSV of 20,000 h^{-1}. The reaction products were analyzed using a quadrupole mass spectrometer. The masses m/e = 4 (He), 28 (N_2 and N_2O), 32 ($^{16}O_2$), 34 ($^{16}O^{18}O$), 36 ($^{18}O_2$), 44 ($N_2{}^{16}O$), and 46 ($N_2{}^{18}O$) were monitored (time resolution ~4 s). He (m/e = 4) was used as a reference in the calibration. The ion current or signal of each mass fragment was converted into a concentration by using calibration factors. The step experiments were corrected for the dead time of the system, which is ~35 s.

The degree of isotope exchange was monitored via the fraction of ^{18}O in the product O_2, $^{18}f = ([^{16}O^{18}O] + 2*[^{18}O_2])/(2*[O_{2,tot}])$. The value of the equilibrium constant of the isotope exchange reaction $^{16}O_2 + {}^{18}O_2 \leftrightarrow 2\ {}^{16}O^{18}O$, $K_e = [^{16}O^{18}O]_2/([^{16}O_2]*[^{18}O_2])$, was also computed. If $K_e = 4$, the distribution of isotopes in O_2 is statistical, i.e. there is a complete equilibration of the oxygen atoms.

2.5. FTIR of NO adsorption

The infrared spectra after NO adsorption of self-supporting wafers (3–5 mg) were recorded at room temperature on a Mattson Galaxy 6020 IR spectrometer with a MCT detector at a resolution of 4 cm^{-1}. The samples were pretreated in situ in 20 mbar O_2 at 673 K for 1 h followed by treatment in vacuum (pressure was lower than 10^{-6} mbar) for another 1 h at either 673 or 873 K. Then the samples were cooled to room temperature in vacuo, followed by room temperature exposure to 5 mbar NO for 30 min. The spectra were recorded at room temperature.

3. Results

3.1. X-ray diffraction (XRD)

Powder XRD measurements were performed in order to check the crystallinity and topology of ZSM-5 after calcination, steaming, and high temperature treatment of the catalysts. Fig. 1 compares the XRD patterns of the parent, Fe-ZSM-5 IE, Fe-ZSM-5 IE-st, and Fe-ZSM-5 IE-HT samples. As can be seen from Fig. 1, all samples maintain the characteristic pattern of the MFI topology. Neither steaming nor treatment in He at 1218 K lead to a measurable decrease in crystallinity. If structural changes took place they must be very much localized and randomly distributed. Also formation of Fe_2O_3 clusters (major reflections expected at 2Θ = 33.2 and 35.7°) was not observed.

3.2. UV–vis spectroscopy

Fig. 2 compares the UV–vis spectra of Fe-ZSM-5 CVD after steaming and calcination. In the spectrum of the Fe-ZSM-5 CVD catalyst the two typical oxygen-to-iron ligand-to-metal charge transfer (LMCT) bands at 44,000 and 37,000 cm^{-1} dominate. The shoulder at 28,000 cm^{-1} is attributed to the presence of oligomeric iron species [31]. The UV–vis spectrum of the corresponding steamed sample (Fe-ZSM-5 CVD-st) is significantly broadened and lower in intensity, indicating the presence of highly distorted and inhomogeneous iron clusters [32]. The appearance of a band at 20,000 cm^{-1} in the steamed sample is due to the formation of Fe_2O_3 clusters. The Fe-ZSM-5 IE catalyst also shows the two ligand-to-metal charge transfer (LMCT) bands around 37,000 and 44,000 cm^{-1}, but no absorption was observed at lower frequencies, which could be attributed to clustered iron species. Fe-ZSM-5 IE contains isolated Fe^{3+} species [33,34] or weakly coupled dimers [31]. After steaming and high temperature treatment the LMCT bands are broadened and their intensity is reduced. The broadening of the LMCT bands indicates a large spread of the energy levels of the metal 3d electrons, i.e., highly distorted and

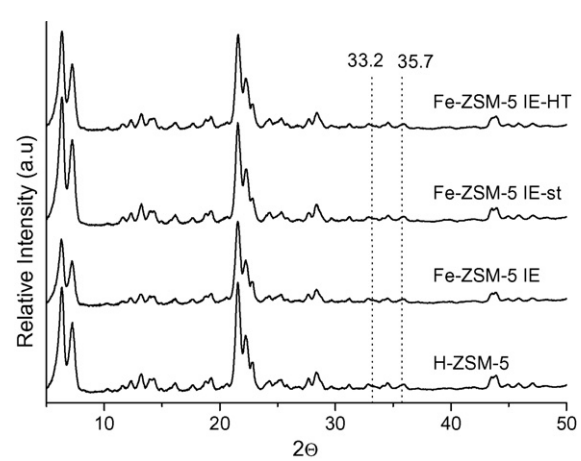

Fig. 1. Powder X-ray diffraction patterns of the parent H-ZSM-5, Fe-ZSM-5 IE, Fe-ZSM-5 IE-st, and Fe-ZSM-5 IE-HT catalysts. The major reflections of Fe_2O_3 are indicated by dotted lines.

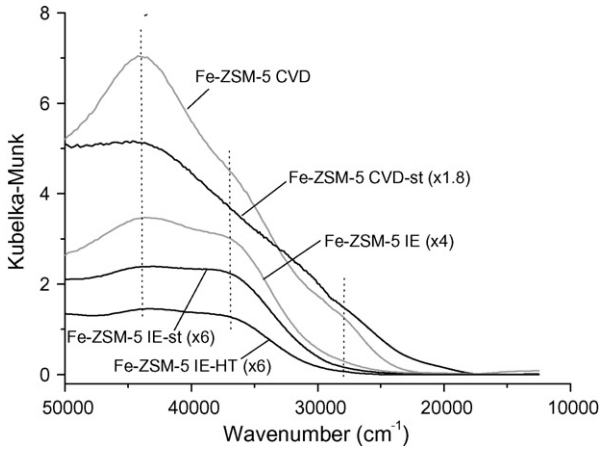

Fig. 2. UV–vis spectra of the Fe-ZSM-5 samples after various treatments. Dotted lines indicate peaks at 44,000, 37,000 and 28,000 cm^{-1}. $BaSO_4$ was used as reference.

inhomogeneous coordination environments of the iron sites. The decrease in intensity is generally ascribed to the reduction of the Fe^{3+} sites to Fe^{2+} [35,36]. No strong absorption around 28,000 cm^{-1} was observed, i.e. no clustering of the iron sites took place during steaming and high temperature treatment of the catalyst.

3.3. FTIR spectroscopy

The FTIR spectra of non-steamed (i.e. calcined), steamed, and high temperature treated Fe-ZSM-5 IE samples in the O–H stretching region are shown in Fig. 3. Bands at 3740 and 3605 cm^{-1} in the non-steamed sample (Fe-ZSM-5 IE) are attributed to external silanol and Brønsted OH groups, respectively. A weak band at 3660 cm^{-1} was observed and assigned to the OH groups connected to extraframework Al. Also Fe–OH groups may contribute to this band [37]. After steaming, the intensity of the Brønsted hydroxyl band decreased significantly. The decrease in the intensity of the Brønsted OH groups after steaming of the Fe-ZSM-5 sample

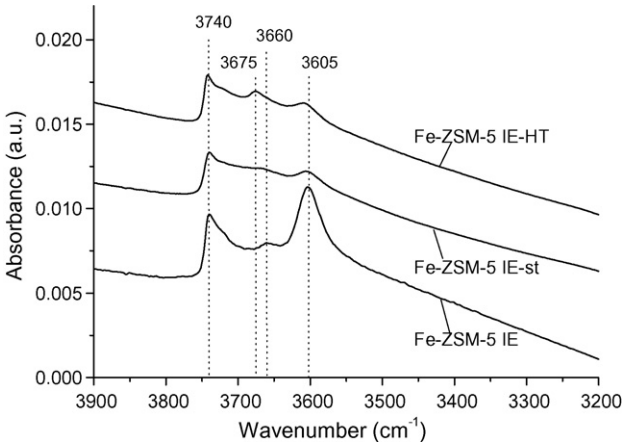

Fig. 3. IR spectra of non-steamed, steamed, and high-temperature treated catalysts. Spectra were recorded at 473 K after degassing at 673 K in He.

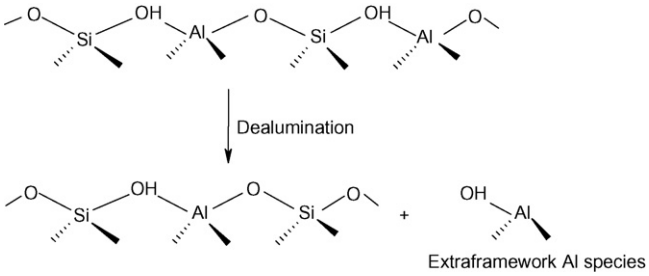

Scheme 1. Dealumination of the zeolite lattice during high temperature treatment.

was reported earlier [7,38] and related to framework dealumination of the sample.

After treatment at 1218 K (Fe-ZSM-5 IE-HT), the intensity of the Brønsted hydroxyl band (at 3605 cm^{-1}) decreased significantly compared to the corresponding calcined catalyst. The intensity of the extraframework Al–OH groups (3660–3675 cm^{-1}) increased after high temperature treatment, due to the migration of Al from the framework to extraframework positions. Also Hensen et al. observed a partial dealumination after calcination at 973 K of the Fe-ZSM-5 catalyst prepared by sublimation of $FeCl_3$ [6,14]. Sobolev et al. found that increasing the calcination temperature from 823 to 1173 K leads to a six-fold decrease in the concentration of Brønsted hydroxyl groups for the H-ZSM-5 with low iron content [1]. The decrease in intensity of the Brønsted hydroxyl band could be due to dealumination (Scheme 1) and/or due to dehydroxylation (Scheme 2) of the zeolite lattice [39,40]. Note that the dehydroxylation of the zeolite lattice is associated with the formation of oxygen vacancies, which are obviously more sensitive to rehydroxylation during exposure to air.

3.4. Activity in steady-state N_2O decomposition

Fig. 4a compares the steady-state N_2O decomposition activity of non-steamed and steamed Fe-ZSM-5 CVD catalysts after pretreatment in He at either 773 K (temperature used for the initial calcination of the sample) or 873 K for 1 h. The steamed catalyst showed a higher steady-state N_2O decomposition activity than the non-steamed catalyst [41]. Moreover, pretreatment at 873 K leads to a higher activity than pretreatment at 773 K [10]. The effect of the pretreatment temperature is larger for the non-steamed than for the steamed

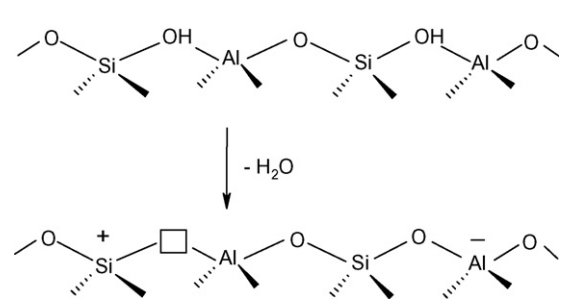

Scheme 2. Dehydroxylation of the zeolite lattice during high temperature treatment. (□) Represents the oxygen vacancies in the lattice.

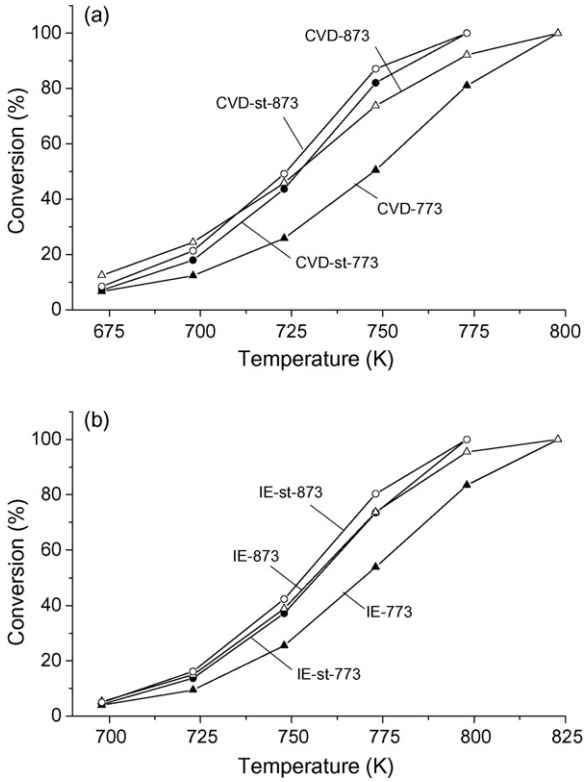

Fig. 4. N_2O decomposition over the non-steamed catalysts after pretreatment at 773 and 873 K (▲ and △) in He and the steamed catalysts after pretreatment at 773 and 873 K (● and ○) in He. (a) over the Fe-ZSM-5 CVD catalysts and (b) over the Fe-ZSM-5 IE catalysts.

sample. Exactly the same trend is observed for the Fe-ZSM-5 sample prepared by ion exchange (Fig. 4b). The first order rate constants and activation energies during N_2O decomposition are listed in Table 1. The activation energies of the steamed catalysts were higher than the corresponding non-steamed catalysts (Table 1), indicating that the steaming changes the nature of the active sites. Further, the comparison between CVD and IE samples shows that the activity of the former is only a factor of 3–4 higher, whereas the iron loading is ten times higher. In the CVD samples a lower fraction of the iron sites takes place in the catalysis because the autoreduction of the CVD samples is thermodynamically less favored [28].

3.5. Isotope exchange and step response experiments

Fig. 5 shows the step response from He to 5000 ppm N_2O in He over the isotopically labeled Fe-ZSM-5 IE at 673 K. A peak of N_2 appears immediately after the step to N_2O. It is due to the reoxidation of Fe^{2+} sites, which were (partly) created by autoreduction during the pretreatment of the catalyst [28,41].

$$2Fe(II) + N_2O \rightarrow 2Fe(III) + O_{catalyst} + N_2 \quad (3)$$

After the N_2 peak stoichiometric N_2O decomposition sets in. The activity of the catalyst immediately reaches steady state (this will not be the case for the pretreatments described below) and remains stable for the duration of the experiment. The

Table 1
Steady-state activity of the calcined and steamed catalysts in N_2O decomposition after pretreatement in He at 773 and 873 K for 1 h. Feed composition: 2500 ppm N_2O, balance He, GHSV = 40,000 h^{-1}

Catalyst	[a]k_{N_2O}	$E_a \pm 10$ (kJ/mol)
Fe-ZSM-5 CVD-773	3.2	139
Fe-ZSM-5 CVD-st-773	6.7	176
Fe-ZSM-5 CVD-873	6.6	129
Fe-ZSM-5 CVD-st-873	7.8	175
Fe-ZSM-5 IE-773	1.1	180
Fe-ZSM-5 IE-st-773	1.9	205
Fe-ZSM-5 IE-873	1.8	181
Fe-ZSM-5 IE-st-873	2.2	207

[a] k_{N_2O}=first-order rate constant at 723 K, in 10^{-4} mol s^{-1} g_{cat}^{-1} bar^{-1}.

isotope equilibrium constant $K_e = [^{16}O^{18}O]^2/([^{16}O_2]*[^{18}O_2])$ is close to 4, which indicates an intensive mixing of the oxygen atoms on the catalyst surface before their desorption as O_2 [42].

The step response drastically changes after pretreatment of the catalyst at 873 K (Fig. 6). The initial peak of N_2, caused by the reoxidation of Fe^{2+} sites, increases (Table 2) indicating that the pretreatment at 873 K leads to more autoreduction. The N_2 peak is followed by a period of high N_2O decomposition activity (called transient activity from now on), which decays to steady state after 10 min. During the transient, the dominating isotopomer of O_2 is $^{16}O_2$. A significantly lower fraction of ^{18}O is incorporated into the O_2 product than in steady state. An analogous behavior was observed for Fe-ZSM-5 CVD after dehydroxylation at 873 K [8].

Fig. 7 shows the step response of the isotopically labeled Fe-ZSM-5 IE-st catalyst after pretreatment at 673 K in He. The

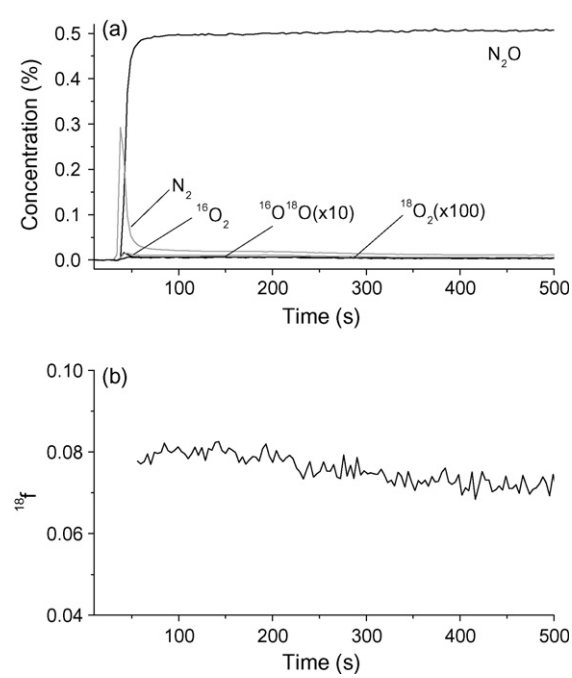

Fig. 5. Response of the Fe-ZSM-5 IE-673 catalyst at 673 K to a step from 0 to 5000 ppm N_2O. The catalyst was reduced with 20% H_2 in He at 673 K, reoxidized with 1% $^{18}O_2$ in He and subsequently treated in He at 673 K. (a) concentration of N_2O, N_2, $^{16}O_2$, $^{16}O^{18}O$ and $^{18}O_2$ and (b) fraction of ^{18}O in O_2.

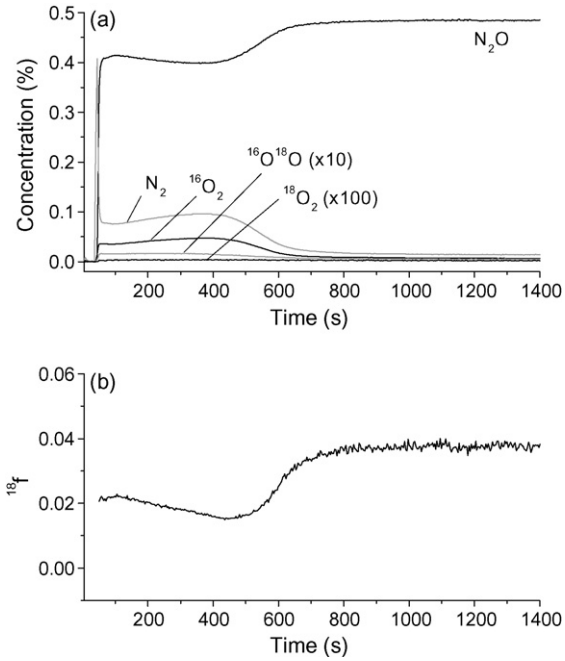

Fig. 6. Response of the Fe-ZSM-5 IE-873 catalyst at 673 K to a step from 0 to 5000 ppm N_2O. The catalyst was reduced with 20% H_2 in He at 673 K, reoxidized with 1% $^{18}O_2$ in He and subsequently treated in He at 873 K. (a) concentration of N_2O, N_2, $^{16}O_2$, $^{16}O^{18}O$ and $^{18}O_2$ and (b) fraction of ^{18}O in O_2.

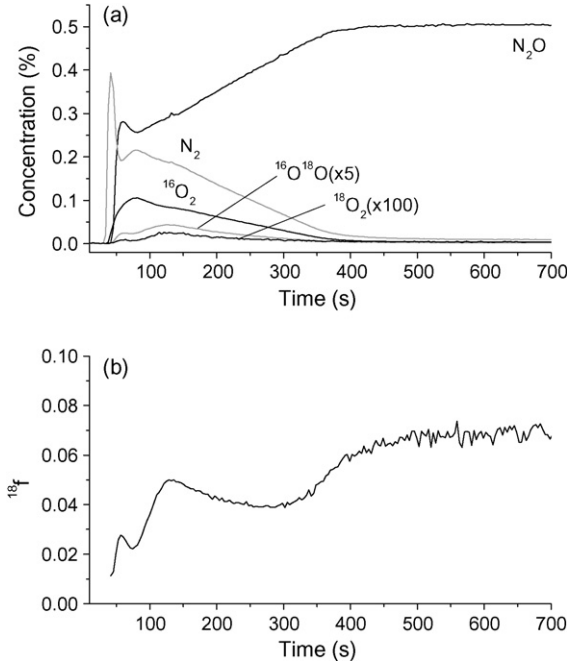

Fig. 7. Response of the Fe-ZSM-5 IE-st-673 catalyst at 673 K to a step from 0 to 5000 ppm N_2O. The catalyst was reduced with 20% H_2 in He at 673 K, reoxidized with 1% $^{18}O_2$ in He and subsequently treated in He at 673 K. (a) concentration of N_2O, N_2, $^{16}O_2$, $^{16}O^{18}O$ and $^{18}O_2$ and (b) fraction of ^{18}O in O_2.

initial peak of N_2, due to the reoxidation of Fe^{2+} sites, is significantly larger than on the corresponding non-steamed catalyst (Table 2). After the N_2 peak we observe a period of high initial N_2O decomposition activity, similar to that of the corresponding non-steamed catalyst after dehydroxylation at 873 K (compare with Fig. 6a). However, the isotope pattern during the transient is very different for the steamed catalyst. In case of the dehydroxylated sample, the fraction of labelled oxygen (^{18}f) in the product O_2 slightly decreased during the transient period until the transient activity decayed and then ^{18}f increased to its steady-state value (see Fig. 6b). The same behavior was also observed for a dehydroxylated Fe-ZSM-5 CVD catalyst [10]. The remarkable difference in case of the steamed catalyst, Fe-ZSM-5 IE-st, is that two maxima of ^{18}f are observed as a function of time. The first maximum of ^{18}f rapidly follows the N_2 reoxidation peak and the second maximum occurs ~100 s later. The Fe-ZSM-5 CVD-st catalyst exhibited qualitatively the same behavior (not shown).

The pattern of ^{18}f described above is typical for all steamed samples that we have tested, irrespective of iron concentration and preparation method. Additional dehydroxylation of the steamed samples at 873 K increases the overall transient activity, but does not change the two-peak pattern of ^{18}f (Fig. 8).

The step response and the pattern of the isotope distribution of the Fe-ZSM-5 IE-HT catalyst after in situ pretreatment at 873 K are very similar to those of the steamed catalyst (Fe-ZSM-5 IE-st) after pretreatment at 873 K (Fig. 9). Like for the steamed catalysts, ^{18}f has two maxima (about 55 and 95 s after the step to N_2O) during the initial phase of the transient reaction (Fig. 9b). Without in situ dehydroxylation at 873 K, Fe-ZSM-5 IE-HT did not exhibit any transient activity. The catalyst reached steady state immediately after the step to N_2O. In both cases, the degree of autoreduction of Fe-ZSM-5 IE-HT was in the same order of magnitude as of the corresponding steamed catalyst.

Table 2
Step response of the non-steamed and steamed catalysts after a step to 5000 ppm N_2O in He at 673 K, following after pretreatment in He at 673 or 873 K

Catalyst	N_2/Fe reoxidation (mol/mol)	N_2/Fe transient (mol/mol)	K_e	Yield N_2 (%) steady state
Fe-ZSM-5 CVD-673	0.016	–	3.8	9.8
Fe-ZSM-5 CVD-st-673	0.023	0.25	3.4	5.3
Fe-ZSM-5 CVD-873	0.025	0.82	3.1	15
Fe-ZSM-5 CVD-st-873	0.027	1.1	2.2	5.8
Fe-ZSM-5 IE	0.16	–	3.8	2.9
Fe-ZSM-5 IE-st	0.25	2.5	1.2	1.8
Fe-ZSM-5 IE-873	0.15	1.8	2.2	2.7
Fe-ZSM-5 IE-st-873	0.26	15	1.1	2.2
Fe-ZSM-5 IE-HT-873	0.23	23.5	0.85	2.1

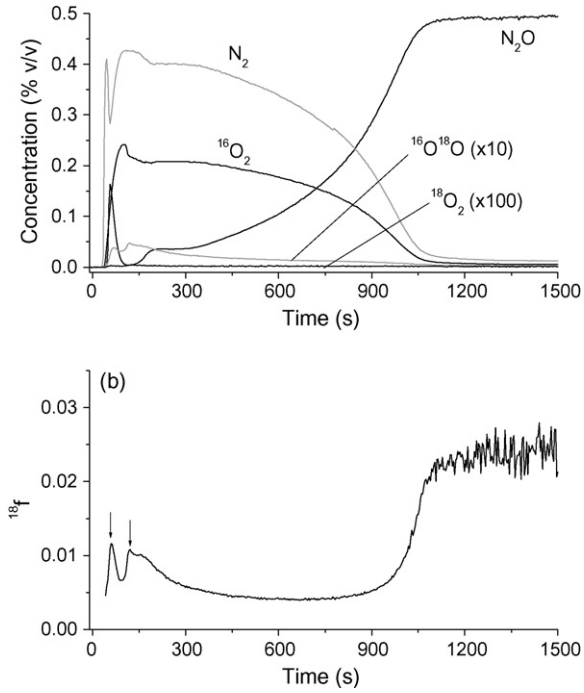

Fig. 8. Response of the Fe-ZSM-5 IE-st-873 catalyst at 673 K to a step from 0 to 5000 ppm N_2O. The catalyst was reduced with 20% H_2 in He at 673 K, reoxidized with 1% $^{18}O_2$ in He and subsequently treated in He at 873 K. (a) concentration of N_2O, N_2, $^{16}O_2$, $^{16}O^{18}O$ and $^{18}O_2$ and (b) fraction of ^{18}O in O_2.

3.6. FTIR of NO adsorption

NO is widely used as a probe molecule to identify the active sites in the catalysts [43–46]. NO preferentially adsorbs on Fe^{2+} sites and forms mono-, di- or trinitrosyl species depending on

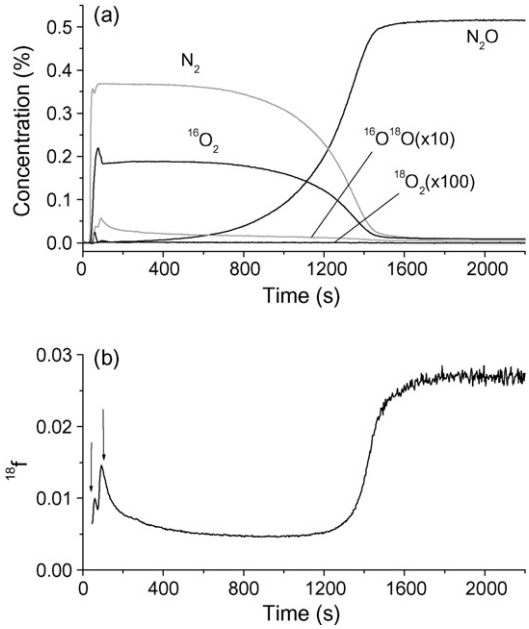

Fig. 9. Response of the Fe-ZSM-5 IE-HT-873 catalyst at 673 K to a step from 0 to 5000 ppm N_2O. The catalyst was reduced with 20% H_2 in He at 673 K, reoxidized with 1% $^{18}O_2$ in He and subsequently treated in He at 873 K. (a) concentration of N_2O, N_2, $^{16}O_2$, $^{16}O^{18}O$ and $^{18}O_2$ and (b) fraction of ^{18}O in O_2.

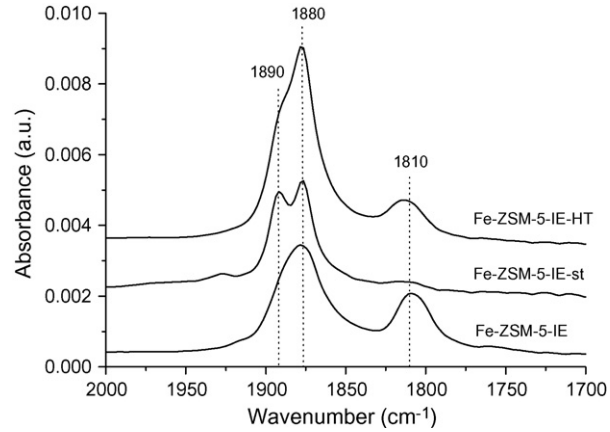

Fig. 10. IR spectra of non-steamed, steamed and high-temperature treated catalysts after room temperature exposure of NO for 30 min. The catalyst was pretreated at 873 K in vacuum.

the available coordination sites. Fig. 10 shows the FTIR spectra of NO adsorbed on the non-steamed, steamed, and high temperature treated Fe-ZSM-5 IE catalysts after pretreatment at 873 K in vacuo. Two bands are observed at 1880 and 1810 cm^{-1} and assigned to mononitrosyl and trinitrosyl species, respectively. Trinitrosyl species are formed on coordinatively unsaturated Fe^{2+} sites, which are generated by the dehydroxylation at 873 K. For the steamed catalyst the amount of trinitrosyl species was lower than for the non-steamed and high temperature treated catalysts. The decrease of trinitrosyl species may be tentatively attributed to a clustering of the iron species due to steaming. An additional mononitrosyl band at higher frequency (at 1890 cm^{-1}) is observed for the steamed catalyst. The shoulder at 1890 cm^{-1} is also observed for the Fe-ZSM-5 HT catalyst. Overall, Fe-ZSM-5 HT has the most intense NO bands and the concentration of coordinatively unsaturated iron species, which give rise to trinitrosyl species, is rather high.

4. Discussion

4.1. Catalyst characterization

A significant framework dealumination of the catalysts took place upon steaming and is evidenced by the decrease in intensity of the Brønsted hydroxyl band at 3605 cm^{-1} (Fig. 3). Zhu et al. observed a similar behavior after steaming of the same type of catalyst. They confirmed the presence of extraframework aluminium by ^{27}Al NMR experiments [6]. Dealumination and/or dehydroxylation also took place during high temperature treatment of Fe-ZSM-5 IE catalyst at 1218 K (Schemes 1 and 2). We cannot clearly distinguish framework dealumination and dehydroxylation, but based on our IR data and on earlier reports in the literature [1,2,40] we suppose that both occur in parallel. Dehydroxylation at high temperature leads to the formation of oxygen vacancies (lattice defects), which could play an important role for the catalytic activity.

Concerning the iron species, steaming leads to a clustering of the iron sites in the case of Fe-ZSM-5 CVD (evidenced by

Table 3
Fraction of labeled oxygen atoms (^{18}f) before and during various steps of N_2O decomposition over the Fe-ZSM-5 catalysts

Catalyst	Before N_2O decomposition	Beginning of transient activity	During steady-state decomposition
Fe-ZSM-5 CVD-673	0.26	–	0.15
Fe-ZSM-5 CVD-st-673	0.49	0.12	0.16
Fe-ZSM-5 CVD-873	0.23	0.12	0.09
Fe-ZSM-5 CVD-st-873	0.21	0.02	0.05
Fe-ZSM-5 IE-673	0.06	–	0.05
Fe-ZSM-5 IE-st-673	0.11	0.03	0.06
Fe-ZSM-5 IE-873	0.03	0.02	0.03
Fe-ZSM-5 IE-st-873	0.04	0.01	0.02
Fe-ZSM-5 IE-HT-873	–	0.01	0.02

UV–vis and EXAFS [41]). For Fe-ZSM-5 IE-st such a clustering is not clearly observed in the UV–vis spectra. The same holds true for Fe-ZSM-5 IE-HT sample. The common feature of the NO absorbed FTIR spectra of Fe-ZSM-5 IE-st and IE-HT is the appearance of the band at 1890 cm^{-1}. This band is a characteristic feature of steamed samples or samples treated at very high temperatures [12,47]. The shift of the NO stretching frequency to higher wavenumber indicates a lower backdonation from Fe, i.e. a lower electron density on the iron sites [45,48]. This indicates that the iron sites are associated with electron withdrawing Al Lewis centers, possibly created by framework dealumination or framework dehydroxylation. Coordinatively unsaturated iron sites (trinitrosyl species) are present in Fe-ZSM-5 IE-HT, but not in the IE-st sample. We can sum up the results as follows: treatment at 873 K dehydroxylates the iron sites; steaming creates electron-deficient iron sites, presumably associated to lattice defects; treatment at 1218 K does both. We find no clear evidence for the formation of iron dimers or clusters after treatment at very high temperatures. The formation of such dimers/clusters was invoked by Yuranov et al. to explain the high activity of the HT treated Fe-ZSM-5 samples [27].

4.2. The effect of steaming and high temperature treatment on the transient reaction

The step response experiments on the isotopically labeled catalysts give very interesting information about the reactivity of the catalysts as a function of their pretreatment. Steaming, dehydroxylation at 873 K, and dehydroxylation at 1218 K all lead to occurrence of transient activity, i.e. a high initial N_2O decomposition activity, which slowly decays to steady state. The isotope distribution (the evolution of ^{18}f) during the transient activity strongly depends on the pretreatment of the catalyst. In order to understand these phenomena more in detail we have to discuss how ^{18}O can be incorporated in the product O_2. N_2O decomposition is carried out with non-labeled N_2O on a catalyst that was partially labeled with ^{18}O (by reduction with H_2 and reoxidation with $^{18}O_2$). The extent of labeling of the active sites is determined by pulsing a small amount of CO before the step to N_2O. CO is oxidized to CO_2 and the fraction of ^{18}O in the product CO_2 is associated with the fraction of ^{18}O at the active sites [49]. The fraction of ^{18}O at the active sites is, in general, higher for CVD than for IE catalysts (Table 3). The pretreatment in He at 873 K redistributes the oxygen species, i.e. labeled extra-lattice oxygen exchanges with non-labeled lattice oxygen and diffuses away from the active sites. This redistribution of labeled oxygen atoms over the lattice reduces the fraction of ^{18}O at the active sites, especially for samples with low iron loading [28]. During the decomposition of N_2O, ^{18}O from the catalyst is incorporated into the product O_2 by exchange of oxygen atoms from the catalyst with the oxygen atoms that N_2O deposits on the active sites. Earlier studies showed that gas phase O_2, once formed, does not exchange with the catalyst surface any more [42].[1]

Our earlier study on Fe-ZSM-5 CVD, dehydroxylated at 873 K, showed that N_2O decomposition during the transient occurs on a single active site [10]. Isotope exchange is limited to the oxygen atoms surrounding the active iron center. As isotope exchange and O_2 desorption proceed the active sites are depleted of ^{18}O and ^{18}f decreases. Then the fast N_2O decomposition on a single iron site decays and the slower steady-state reaction becomes dominant. Steady-state N_2O decomposition occurs via the migration of oxygen atoms deposited on separate iron centers. The migration of the deposited oxygen atoms over the catalyst involves an intensive exchange with oxygen atoms from the catalyst and leads to the increase of ^{18}f when the transient activity decays. These trends are reproduced on the Fe-ZSM-5 IE catalyst, which was dehydroxylated at 873 K.

The situation is different for steamed catalysts. Instead of slowly decreasing with time (until transient activity decays), ^{18}f has two maxima at the beginning of the transient. The first peak is attributed to the labeled oxygen atoms that are directly associated with the active iron centers. They are incorporated into the product O_2 by exchange reactions. Exchange and O_2 desorption rapidly deplete this pool and therefore ^{18}f decreases. Then a second pool of (labeled) oxygen atoms becomes involved in the reaction and makes ^{18}f rise again. This pool is slowly depleted and then the steamed catalyst follows the behavior of the dehydroxylated sample.

[1] The absence of isotope exchange with O_2 differs from the results of Novakowa et al., obtained in a batch reactor [50]. In our opinion, the discrepancy between the two results is not unreasonable. The dissociation of O_2 on the catalyst is slower than the dissociation of N_2O. In a flow reactor with short contact times, the faster reaction will be strongly favored while in a batch reactor both will occur after long reaction times.

In order to describe the mechanism in more detail on a molecular level we would need to know the structure of the active site. Unfortunately, at present date the nature of extraframework species in steamed samples remains unresolved. We can, however, speculate on the structure of the active site in the HT-treated catalysts: Let us assume that the active site is a single Fe^{2+} cation (while not ruling out that a similar mechanism may be possible for iron dimers). In order to be easily accessible to reactants the Fe^{2+} cation should be located in the 10-membered ring channels of ZSM-5. For Cu-ZSM-5 with a mixed oxidation state of Cu(I)/Cu(II) two preferred cation locations in the 10-membered ring channel were recently identified by XRD [51]. One of them is associated with a single T-site, the other is located in a 5-memberd ring. The two charges of Fe^{2+} are more easily compensated in a 5-membered ring and we suspect this to be the preferred location of the iron cations. Further, the characterization data indicate that Fe^{2+} is located next to strongly electron-withdrawing Al centers, associated with lattice defects. For reasons of charge balancing, these lattice defects are probably not located directly in the ring where Fe^{2+} is stabilized, but in a neighboring ring. In that case we can interpret the two maxima in ^{18}f as follows: The first oxygen pool is associated with the oxygen atoms of the ring where Fe^{2+} is located. Scheme 3 indicates how isotope exchange reactions within the ring are possible during the cycle of N_2O decomposition. Due to the high mobility of the oxygen species, also more distant lattice oxygen atoms (which are partially labeled) start to migrate towards the active site. These migrating oxygen atoms are first trapped by the neighboring defect before reaching the ring where Fe^{2+} is located. The trapping of migrating oxygen atoms by the defect can explain the minimum in ^{18}f.

Apart from this particularity, the mechanism of Scheme 3 is very similar to the one proposed in our earlier work [10]. It also fits well with a recent TAP study of Kondratenko and Perez-Ramirez [52]. The very high activity of the steamed or HT-treated samples during the transient period leads to a very rapid desorption of O_2. The rapid desorption leaves the oxygen atoms less time to undergo isotope exchange. Therefore, the ^{18}f fraction remains very low during the transient period (see Table 3).

We also have to discuss why the transient activity decays to steady state. In our earlier work we proposed that transient activity was entirely related to the dehydroxylation of the iron sites [10]. The dehydroxylation creates open coordination sites and allows two oxygen atoms from N_2O to adsorb on a single iron site, which allows rapid desorption of O_2. This mechanism decays as the active sites become slowly rehydroxylated by traces of H_2O in the feed. For the steamed catalysts this explanation is not applicable. They exhibit transient activity without prior treatment at 873 K. The high initial activity is therefore an inherent feature of the active sites in the steamed catalyst and not related to dehydroxylation. The question then arises why the transient activity decays. Rehydroxylation by traces of H_2O in the feed cannot be the reason. The structure of the active sites must change during the course of the reaction. Perez-Ramirez et al. recently showed that the oxygen atoms that N_2O deposits on the active sites are rapidly transformed into a less active surface species unless they are given the possibility to react immediately [53–55]. This transformation into a less active surface species and/or the healing of defects may be responsible for the decay of the transient activity in the steamed/HT-treated catalysts. The deactivation of the transient activity is, however, not irreversible. A simple purge in inert gas at 673 K can, partially, restore the high initial activity if the step to N_2O is repeated.

4.3. The effect of steaming and high temperature treatment on the steady-state activity

The transient experiments, which we discussed above, show that steaming and high temperature pretreatment qualitatively changes the nature of the active sites. This is probably related to the creation of iron sites next to electron-withdrawing Al Lewis

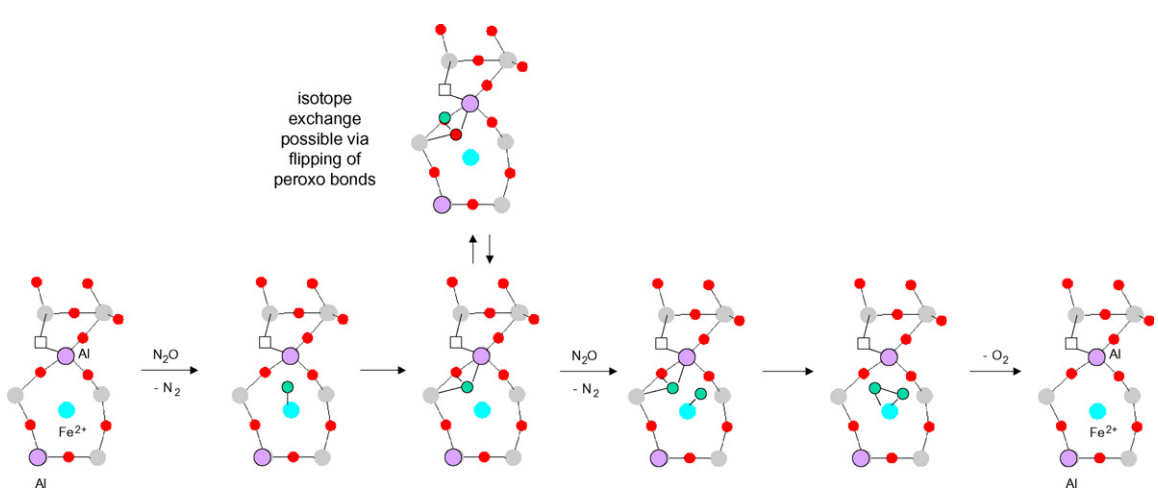

Scheme 3. Scheme of the catalytic cycle during the transient period. A hypothetical structure of an isolated Fe^{2+} cation next to a lattice defect is used for illustration. We chose a plausible distribution of bonds in the intermediate structures, but other mesomeric structures and/or other distributions of the oxygen atoms over the ring are certainly possible. Note that the reaction scheme is purely hypothetical. It is meant as guide for the chemists' imagination.

sites, which was created by the creation of framework defects. The question arises whether these sites have an intrinsically higher activity in N_2O decomposition. The tentative answer is no. The changes in N_2O decomposition activity upon steaming and dehydroxylation can be largely ascribed to their effect on the autoreduction of the iron species. The TOF (N_2O activity per initial concentration of Fe^{2+} sites) does not change significantly upon steaming or HT treatment. The steamed and HT treated samples behave differently only during the initial phase of the reaction, i.e. during the transient period. Then a rearrangement of the catalyst surface takes place and in steady-state N_2O decomposition at 673 K, the active sites generated by the high temperature pretreatments seem to have lost their particularity. We attribute this to the fact that the rate of N_2O decomposition is limited by O_2 desorption and not by the dissociation of N_2O. The mobility of the surface oxygen atoms is more important in N_2O decomposition than their intrinsic activity. In reaction with other reductants (benzene, NO, CH_4, etc.), the turnover frequency may very well change since the reaction regime will resemble more the one observed during the transient reaction.

5. Conclusions

Steaming and treatment of Fe-ZSM-5 at very high temperatures lead to the creation of localised defects in the ZSM-5 framework. The electronic properties of the iron sites in the vicinity of these defects change, which is evidenced by the shift of mononitrosyl band to the higher frequencies. These iron sites in the vicinity of defects exhibit a qualitatively different behavior in N_2O decomposition. The difference is observed, however, only in the initial phase of the reaction during which the catalyst exhibits a higher activity than in steady state.

In steady state the turn-over-frequency of the aforementioned iron sites is not significantly different from other Fe-ZSM-5 catalysts, which did not undergo steaming or high temperature dehydroxylation. The increase of activity following these pretreatments can be explained by an increase in the number of active sites, as a consequence of autoreduction of the iron centers during the pretreatment. The intrinsic activity per site, however, does not change much. This may be due to the fact that the rate-limiting step of N_2O decomposition is not the activation of N_2O, but the formation of O_2.

References

[1] V.I. Sobolev, K.A. Dubkov, E.A. Paukshtis, L.V. Pirutko, M.A. Rodkin, A.S. Kharitonov, G.I. Panov, Appl. Catal. A 141 (1996) 185.
[2] L.M. Kustov, A.L. Tarasov, V.I. Bogdan, A.A. Tyrlov, J.W. Fulmer, Catal. Today 61 (2000) 123.
[3] K.A. Dubkov, N.S. Ovanesyan, A.A. Shteinman, E.V. Starokon, G.I. Panov, J. Catal. 207 (2002) 341.
[4] A. Ribera, I.W.C.E. Arends, S. de Vries, J. Pérez-Ramirez, R.A. Sheldon, J. Catal. 195 (2000) 287.
[5] L.V. Pirutko, V.S. Chernyavsky, A.K. Uriarte, G.I. Panov, Appl. Catal. A 227 (2002) 143.
[6] Q. Zhu, B.L. Mojet, R.A.J. Janssen, E.M.J. Hensen, J. van Grondelle, P.C.M.M. Magusin, R.A. van Santen, Catal. Lett. 81 (2002) 205.
[7] P. Kubanek, B. Wichterlova, Z. Sobalik, J. Catal. 211 (2002) 109.
[8] J. Jia, K.S. Pillai, W.M.H. Sachtler, J. Catal. 221 (2004) 119.
[9] V.L. Zholobenko, Mendeleev Commun. 3 (1993) 28.
[10] P.K. Roy, G.D. Pirngruber, J. Catal. 227 (2004) 164.
[11] J.F. Jia, B. Wen, W.M.H. Sachtler, J. Catal. 210 (2002) 453.
[12] K. Sun, H. Xia, E. Hensen, R. van Santen, C. Li, J. Catal. 238 (2006) 186.
[13] J. Pérez-Ramirez, F. Kapteijn, J.C. Groen, A. Doménech, G. Mul, J.A. Moulijn, J. Catal. 214 (2003) 33.
[14] Q. Zhu, R.M. van Teeffelen, R.A. van Santen, E.J.M. Hensen, J. Catal. 221 (2004) 575.
[15] J. Novakova, Z. Sobalik, Catal. Lett. 89 (2003) 243.
[16] J. Perez-Ramirez, F. Kapteijn, G. Mul, J.A. Moulijn, Catal. Commun. 3 (2002) 19.
[17] Z. Sobalik, P. Kubanek, O. Bortnovsky, A. Vondrova, Z. Tvaruzkova, J.E. Sponer, B. Wichterlova, Stud. Surf. Sci. Catal. 142 (2002) 533.
[18] D. Kaucky, Z. Sobalik, M. Schwarze, A. Vondrova, B. Wichterlova, J. Catal. 238 (2006) 293.
[19] E.J.M. Hensen, Q. Zhu, R.A. van Santen, J. Catal. 220 (2003) 260.
[20] E.J.M. Hensen, Q. Zhu, R.A.J. Janssen, P.C.M.M. Magusin, P.J. Kooyman, R.A. van Santen, J. Catal. 233 (2005) 123.
[21] E.J.M. Hensen, Q. Zhu, R.A.v. Santen, J. Catal. 233 (2005) 136.
[22] F. Kollmer, H. Hausmann, W.F. Holderich, J. Catal. 227 (2004) 398.
[23] F. Kollmer, H. Hausmann, W.F. Holderich, J. Catal. 227 (2004) 408.
[24] K. Sun, H. Zhang, H. Xia, Y. Lian, Y. Li, Z. Chi, P. Ying, C. Li, Chem. Commun. (2004) 2480.
[25] G. Centi, S. Perathoner, R. Arrigo, G. Giordano, A. Katovic, V. Pedula, Appl. Catal. A 307 (2006) 30.
[26] G. Centi, C. Genovese, G. Giordano, A. Katovic, S. Perathoner, Catal. Today 91/92 (2004) 17.
[27] I. Yuranov, D.A. Bulushev, A. Renken, L. Kiwi-Minsker, J. Catal. 227 (2004) 138.
[28] G.D. Pirngruber, P.K. Roy, R. Prins, J. Catal. 246 (2007) 147.
[29] H.Y. Chen, T. Voskoboinikov, W.M.H. Sachtler, J. Catal. 180 (1998) 171.
[30] G.D. Pirngruber, J. Catal. 219 (2003) 456.
[31] G.D. Pirngruber, P.K. Roy, R. Prins, Phys. Chem. Chem. Phys. 8 (2006) 3939.
[32] A.M. Ferretti, C. Oliva, L. Forni, G. Berlier, A. Zecchina, C. Lamberti, J. Catal. 208 (2002) 83.
[33] H.H. Tippins, Phys. Rev. B 1 (1970) 126.
[34] G. Lehmann, Z. Phys. Chem. Neue Folge 72 (1970) 279.
[35] J. Pérez-Ramirez, M.S. Kumar, A. Brückner, J. Catal. 223 (2004) 13.
[36] M.S. Kumar, M. Schwidder, W. Grünert, U. Bentrup, A. Brückner, J. Catal. 239 (2006) 173.
[37] S. Bordiga, R. Buzzoni, F. Geobaldo, C. Lamberti, E. Giamello, A. Zecchina, G. Leofanti, G. Petrini, G. Tozzola, G. Vlaic, J. Catal. 158 (1996) 486.
[38] J. Pérez-Ramirez, G. Mul, F. Kapteijn, J.A. Moulijn, A.R. Overweg, A. Doménech, A. Ribera, I.W.C.E. Arends, J. Catal. 207 (2002) 113.
[39] M.H.W. Sonnermans, C. Heijer, M. Crocker, J. Phys. Chem. 97 (1993) 440.
[40] I. Balint, M.A. Springuel-Huet, K. Aika, J. Fraissard, Phys. Chem. Chem. Phys. 1 (1999) 3845.
[41] G.D. Pirngruber, M. Luechinger, P.K. Roy, A. Cecchetto, P. Smirniotis, J. Catal. 224 (2004) 429.
[42] G.D. Pirngruber, P.K. Roy, Catal. Lett. 93 (2004) 75.
[43] G. Berlier, G. Spoto, S. Bordiga, G. Ricchiardi, P. Fisicaro, A. Zecchina, I. Rossetti, E. Selli, L. Forni, E. Giamello, C. Lamberti, J. Catal. 208 (2002) 64.
[44] G. Berlier, G. Spoto, G. Ricchiardi, S. Bordiga, C. Lamberti, A. Zecchina, J. Mol. Catal. A 182 (2002) 359.
[45] G. Berlier, A. Zecchina, G. Spoto, G. Ricchiardi, S. Bordiga, C. Lamberti, J. Catal. 215 (2003) 264.
[46] G. Mul, J. Perez-Ramirez, F. Kapteijn, J.A. Moulijn, Catal. Lett. 80 (2002) 129.
[47] I. Yuranov, D.A. Bulushev, A. Renken, L. Kiwi-Minsker, Appl. Catal. A Gen. 319 (2007) 128.
[48] G. Berlier, G. Ricchiardi, S. Bordiga, A. Zecchina, J. Catal. 229 (2005) 127.
[49] K.Y.S. Tanaka, S. Ito, S. Kameoka, K. Kunimori, J. Catal. 200 (2001) 203.

[50] J. Novakova, M. Schwarze, Z. Sobalik, Catal. Lett. 104 (2005) 157.
[51] B.F. Mentzen, G. Bergeret, J. Phys. Chem. C 111 (2007) 12512.
[52] E.V. Kondratenko, J.P. Pérez-Ramírez, J. Phys. Chem. B 110 (2006) 22586.
[53] E.V. Kondratenko, J. Pérez-Ramírez, Appl. Catal. A 267 (2004) 181.
[54] J. Pérez-Ramírez, E.V. Kondratenko, M.N. Debbagh, J. Catal. 233 (2005) 442.
[55] E.V. Kondratenko, J. Perez Ramirez, Appl. Catal. B 64 (2005) 35.